Iranian Journal of Materials Science and Engineering, Vol. 20, Number 3, September 2023
RESEARCH PAPER

Mechanical and Microstructural Evaluation of Recycled 7075 Aluminum Swarf

Mohammad Porhonar[1], Yazdan Shajari[2], Seyed Hossein Razavi[3], Zahra-Sadat SeyedRaoufi[1,*]

* *z.seyedraoufi@kiau.ac.ir*

[1] Department of Materials Science and Engineering, Islamic Azad University, Karaj Branch, Karaj, Alborz, Iran
[2] Materials and Energy Research Center, Meshkindasht, Alborz, Iran
[3] School of Metallurgy and Materials Engineering, Iran University of Science and Technology, Tehran, Iran

Received: November 2021 **Revised: July 2023** **Accepted: August 2023**
DOI: 10.22068/ijmse.2578

Abstract: *In this research, after pressing in a cylindrical mold, the AA 7075 alloy swarf was melted and cast in a wet sand mold. After rolling and cutting, sheets with two different thicknesses of 6 and 20 mm were obtained. The sheets after homogenization were solutionized at 485°C for 30 and 90 minutes, respectively, due to differences in thickness and thermal gradients. The solutionized samples were quenched in 3 polymer solutions containing 10, 30, and 50% Poly Alekylene Glycol. The results showed that melting, casting, rolling, and heat treatment of AA7075 alloy swarf with similar properties to this alloy is achievable. Microstructural studies by optical microscopes (OM), Field Emission Scanning Electron Microscopy (FESEM), and X-ray diffraction (XRD) showed that by increasing the quenching rate after the solutionizing process, precipitation increases during aging. The tensile test results indicated that as the quench rate and internal energy increase, the diffusion driving force would increase the precipitation of alloying elements. Hence, this leads to an increase in hardness and a reduction of its strain after aging.*

Keywords: *Aluminum, 7075, Swarf, Casting, Heat Treatment, Mechanical Properties.*

1. INTRODUCTION

Optimal mechanical properties of aluminum alloys are obtained by alloying elements, heat treatment, and, consequently, the formation of precipitates, which create barriers that limit the movement of dislocations. AA 7075 is one of the aluminum alloys with excellent properties such as low density, high strength, toughness, and fatigue resistance. Moreover, it has been used in various structures. This alloy is widely used in aerospace structures and all structures requiring high-stress resistance [2, 3].

The AA7075 is heat treatable, and the primary mechanism of its strength comes by the formation of $MgZn_2$ precipitates with the 2 to 1 ratio of Zn to Mg. Aluminum alloys are heat-treated in three stages, solutionizing, quenching, and aging. Solutionizing involves placing the alloy at the right temperature and time to achieve a homogeneous, single-phase state. After Solutionizing to obtain a supersaturated solid solution, the alloy will be quenched in diverse cooling environments such as water, mixtures of the water and polymer, oil, and air [2]. A different cooling rate is suggested for each alloy. Also, High cooling rates cause the formation of unwanted phases or very high residual stresses, which eventually lead to distortion [3, 4].

In 7XXX series aluminum alloys, Zn has a high solubility in the matrix and does not adversely affect the microstructure. The 7xxx aluminum series includes Mg, Zn, Cu, and additional elements such as Cr, Mn, Zr, and sometimes Fe and Si [5]. In the AA7075 casting alloy, precipitates such as $(Fe, Cr)_3SiAl_{12}$, Mg_2Si, $MgZn_2$, and Al-$MgZn_2$ can be observed in which other phases are more likely a combination of Al and Cu as an alternative to $MgZn_2$. These phases could be considered $Mg(Zn, Cu, Al)_2$, which are convertible to iron-rich phases like Al_7Cu_2Fe as the temperature increases. It is noteworthy that the Mg_2Si phase is relatively insoluble during the heat treatment process and will become spherical by diffusion [6, 7]. According to previous research, AA7075 samples in different cooling environments comprise two phases α, and β, which are physically distinct and separated by fuzzy boundaries. The precipitation process is not instant and involves secondary nucleation caused by thermal fluctuation and reaching a steady-state [8-10]. AA7075 age-hardening is associated with the formation of GP zones, which are almost circular. As the time of age-hardening increases, these areas become bigger and eventually end up forming alloying precipitates. GP zones

[DOI: 10.22068/ijmse.2578]

containing high levels of Zn and Mg become precipitates called η' and M'. If the amount of Zn and Mg becomes higher than 2.2, $MgZn_2$ and Mg_3Zn_3Al precipitates are more likely to form in the presence of copper (Table 4) [7].
The effect of precipitates on mechanical properties usually comes from reheating the quenched part to temperatures between 95°C and 205°C. The structural alterations that occur at elevated temperatures are different from room temperature. A distinctive feature of age-hardening effects on tensile properties can be more yield strength over tensile strength, which reduces malleability. Therefore, alloys with T6 heat treatment will have higher strength and less malleability than T4 [6, 7]. 7XXX Series alloys are not stable in natural aging. The strength will increase with the growth of GP zones over the years. However, artificial aging and elevated temperature have stable properties such as high strength, excellent corrosion resistance, and low crack growth rate. Usually, 115°C to 120°C temperature is used to obtain the T6 hardness characteristic, which is less time-consuming, more stable, and produces high strength [6, 7, and 9].
Polyalkylene Glycol (PAG) has been used in aluminum to create a balance between water and oil, prevent vapor film formation, and reduce temperature tolerance around parts [6]. As the PAG percentage in water increases, the cooling rate decreases. PAG is usually added to the water to adjust the residual stress and the maximum cooling rate [12]. As stated, quenching by water, the vapor film will form around parts and leads to an inhomogeneous heat transfer, which by adding PAG to the water, this vapor film will remove, and the temperature around parts reduce homogeneously. As a result, it reduces residual stress and distortion [11 and 12].
The purpose of this study is to investigate whether the swarf of AA7075 machined plates could be recycled, and cast, and does it obtain appropriate mechanical properties from heat treatment.

2. EXPERIMENTAL PROCEDURES

In this study, initially, after putting the swarf into an oven to draw out moister AA7075 swarf, which was produced from the machining process, Fig. 1, was pressed into the H13 heat-treated cylindrical mold steel with 30 mm diameter and 20 cm height and 400 MPa Bar pressure. The pressed parts were melted in a "Control Switch" induction furnace with 100 kg capacity while magnetically stirred to prevent aluminum oxides from trapping inside the melt. Besides, in the first step, swarfs were annealed for one hour at 500ºC under HF gas to deoxidize them. During casting, after ensuring the homogeneity of the melt, Martini N71P degasser tablets were placed in aluminum foil and held by a holder at the bottom of the cast to complete the deoxidation and degassing process. Afterward, the molten swarf was cast in a sand mold with 20x20x10 cm dimension. The chemical composition of the machined bar and the casted ingot was obtained by the UV-vis-double-beam-spectrophotometer Model-U2900, as shown in Table 1. This table shows that the chemical composition of the fragment complies with the AA7075 standard composition according to ASTM B209M-14 [13]. It is mentioned in the references that no alloying elements waste will be caused if separation and classification of AA7075 are carried out before melting and casting [8]. Hence, if the chemical composition of the used swarf is assured, there will be no change in the chemical composition of the final part. For this purpose, the spectrometry test was used before and after machining.

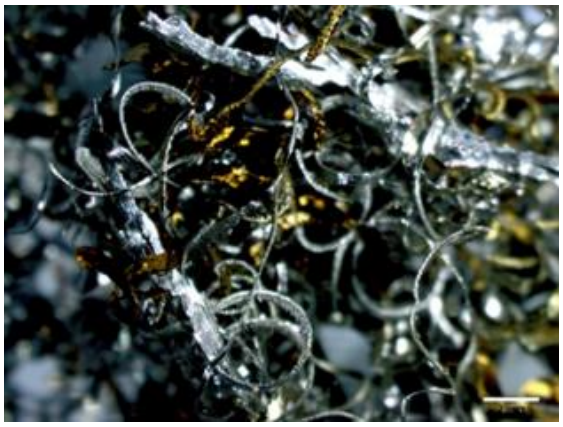

Fig. 1. AA 7075 swarf produced from the machining process

The ingots were cut into 8- and 22- mm thicknesses using a metal cutting bandsaw. Then, by performing five steps using a rolling machine, thicknesses of 6 and 20 mm were obtained.
The samples were cut into 200 × 200 mm, including three 20 mm thick samples and three 6 mm thick samples [11–14]. A total of 10 samples were set aside, including six targets and four blank samples, as shown in Table 2. The samples were homogenized according to the ASTM B918

[DOI: 10.22068/ijmse.2578]

standard in a Heat resistant furnace equipped with k type thermocouple. Samples first were put at 417°C for 3 hours then cooled at 52°C every 1 hour to reach 212°C after that, stayed at 212°C for 3 hours, and finally were cooled in the air to provide homogeneous heat-transformation.

After homogenization, samples were solutionized according to ASTM B918 and Table 3 [11]. 6 and 20 mm samples were solutionized at 485°C for 30 and 95 minutes, respectively. Afterward, samples were quenched in three liquid polymer solutions, which are water-based and can be solved in water, with different percentages of polymer in water, including 10%, 30%, and 50%. After reaching room temperature, samples were stored at -21°C to prevent microstructural changes. Based on standards, samples can be stored at -21°C for 90 days after quenching to prevent microstructural alterations [6].

Vickers hardness test was performed using Instron Wolpert with 40 N force. After conducting stages mentioned on six target samples, the age-hardening process was carried out. The AA7075-T6 age-hardening was carried out according to the ASTM B918 standard [13] at 121°C for 24 hours, according to Table 3, and then cooled at room temperature. Microstructural studies were carried out before and after age-hardening using optical microscopy (OM), X-ray Diffraction (XRD) with a scanning speed of 0.05 degrees per second and with an X-ray wavelength of 1.55566 copper angstrom by PHILIPS diffractometer model PW1730, and Scanning Electron Microscopy (SEM) made in the Czech Republic VEGA/TESCAN model equipped with Energy Diffraction Spectroscopy (EDS).

Table 1. Chemical composition of AA7075 (Wt. %).

Standard Sample	Cast Sample	Rod	Element
Base	Base	Base	Al
5.100 - 6.100	5.900	5.895	Zn
- 2.900 - 2.100	2.630	2.429	Mg
1.200 - 2.000	1.210	1.215	Cu
0.180 – 0.280	0.250	0.198	Cr
0.500 >	0.340	0.330	Fe
0.400 >	0.100	0.092	Si
0.300 >	0.160	0.158	Mn
0.200 >	0.055	0.050	Ti

Table 2. Coding and Heat treatment stages.

Samples Coding	Thickness (mm)	Homogenizing Condition	Solutionizing (Celsius)	Quenchant solution
A	6	–	–	–
B	20	–	–	–
C	6	417˚C for 10 Hour	–	–
D	20	417˚C for 10 Hour	–	–
E	6	417˚C for 10 Hour	485 for 30 minutes	10% Polymer 90% water
F	20	417˚C for 10 Hour	485 for 95 minutes	10% Polymer 90% water
G	6	417˚C for 10 Hour	485 for 30 minutes	30% Polymer 70% water
H	20	417˚C for 10 Hour	485 for 95 minutes	30% Polymer 70% water
I	6	417˚C for 10 Hour	485 for 30 minutes	50% Polymer 50% water
J	20	417˚C for 10 Hour	485 for 95 minutes	50% Polymer 50% water

Table 3. Homogenizing and solutionizing of 7075, according to ASTM B918 [2].

Heat-treatment	Homogenizing		Solutionizing		Age Hardening			
	Temperature (˚c)	Hint	Metal Temperature (˚c)	Quenchant Temperature (˚c)	Metal Temperature (˚c)	Time (h)	Type	Hint
Plates	417	W^u	460-499	44	121	24	T6	W^u
W^u: The temperature rising to 570˚c must be staged, every hour 12˚c.								

[DOI: 10.22068/ijmse.2578]

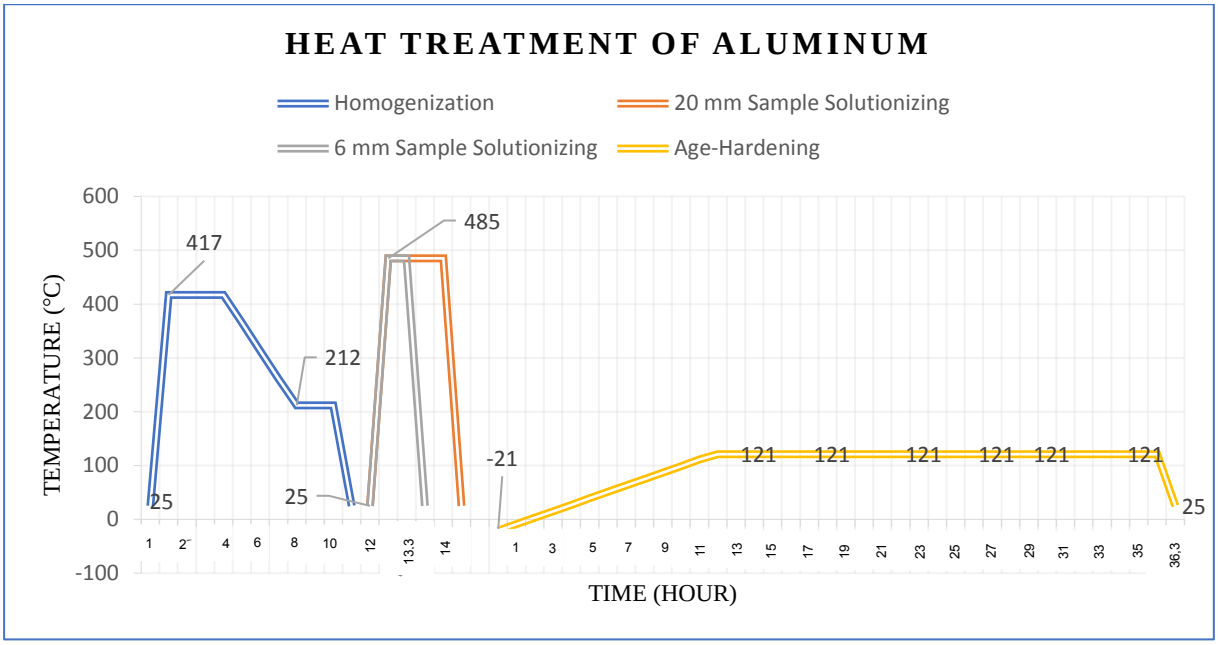

Fig. 2. The diagram of the heat treatment process including homogenization, quenching, and age-hardening of AA 7075-T6

To evaluate the yield strength, strain diagram, and mechanical characteristics of samples, the tensile test was carried out by the Go-Tech 7052-D30 based on the ASTM B557 standard at 25°C and 41% humidity with a length of 165 mm and width of 13 mm, with a gauge length of 50 mm.

3. RESULTS AND DISCUSSION

Fig. 3 shows the metallographic structure of recycled 7075 aluminum alloys. As seen from Fig. 3-a the as-cast structure is composed of dendritic matrix phase and interdendritic low-melting point eutectic phase. After homogenizing annealing at 470°C for 24 h, most of the interdendritic phases in the as-cast structure are dissolved in the matrix (Fig 3-b), and the dendrite segregation is significantly improved. Due to holding for a long time, the atoms in the alloy are fully diffused, and the heterogeneity in chemical composition and microstructure is eliminated, resulting in the improvement for the plastic deformation ability of the alloy [14].

The metallographic structure of recycled 7075 aluminum alloy plates is shown in Fig. 3-c. It can be seen that the recycled 7075 aluminum alloys obtained a proper microstructure with $MgZn_2$ as a main hardening phase. In addition, it can be also seen that the precipitated impurity phases cannot be eliminated thoroughly after heat treatment.

Fig. 4 illustrates the results of the polymeric cooling media on hardness. In 6-mm samples, as the cooling rate decline, hardness decreases while 20 mm sample in the highest cooling rate, 10% polymer solution, has the lowest hardness. Due to the hardness number, it can be deduced that a 10% polymer solution creates a better supersaturated solid-solution than the 30% and 50%. In the 6-mm samples, before and after aging, as the cooling rate decreases, hardness also experiences a reduction, while in the 20-mm samples, before and after aging, hardness initially increased and then decreased by decreasing cooling rate.

During Solutionizing and quenching, after the metal is brought to pre-eutectic temperature and maintained at that temperature, precipitates are homogeneously dissolved and formed. Quenching the object creates a homogeneous supersaturated solid solution so that precipitates can be prepared for the hardening stage. The driving force of supersaturated solution increases precipitates' formation, although other factors such as the cooling rate and atoms' mobility can be influential [7].

The number of $MgZn_2$, $Mg_3Zn_3Al_2$, and Mn_5ZnAl_{24} precipitates by studying the formation of precipitates before homogenization shows which are small in size and gray and black, among large black precipitates which appear to be Mg_2Si. Also, small black precipitates are most likely to

[DOI: 10.22068/ijmse.2578]

be Cr, Fe, and Mn. The reason behind the large Mg_2Si precipitates could be the non-dissolving of this phase during the solutionizing and quenching, which resulted in their growth by diffusion. As a result of the Mn, Cr, and Zr entities in the AA7075 matrix, this alloy is not sensitive to quenching. Therefore, low quench rate media such as boiling water, oil, and air do not affect the mechanical properties of this alloy, and it will also reduce the stress corrosion resistance [3, 14].

In low percentages of polymer in water, which declines the cooling rate, alloying elements do not have the opportunity to diffuse and form precipitates such as $MgZn_2$, $Mg_3Zn_3Al_2$, and Mn_5ZnAl_{24}. This could stem from their low quantity in solid solution which can be seen from XRD results in Fig. 5-A and C. The results of EDS and investigation through OM results in Fig. 5 (A) and (B) and the XRD pattern (Fig. 5-C) indicate that the alloying elements did not diffuse, and black particles are Si, Fe, and Cr compounds.

By studying the pre-aging conditions and observing the effects of incomplete recrystallization, the grain size appears to increase, and no new GP regions have formed, so grains continued to grow [6]. The increase in grain size can be attributed to the lack of driving force required to complete the recrystallization process.

As the cooling rate decreases due to increasing the polymer content in water to 30% and, consequently, a reduction in internal energy after the quench, no significant change in the alloying elements' diffusion happened. Moreover, most of the alloying elements, shown in the XRD pattern of Fig. 6, are dissolved in the field, so there is no trace of $MgZn_2$, $Mg_3Zn_3Al_2$, and Mn_5ZnAl_{24} compounds in the field. Due to the homogeneous positioning of the precipitates and elements in Fig. 7, it can be deduced that a suitable supersaturated solution was produced in both 6- and 20-mm samples.

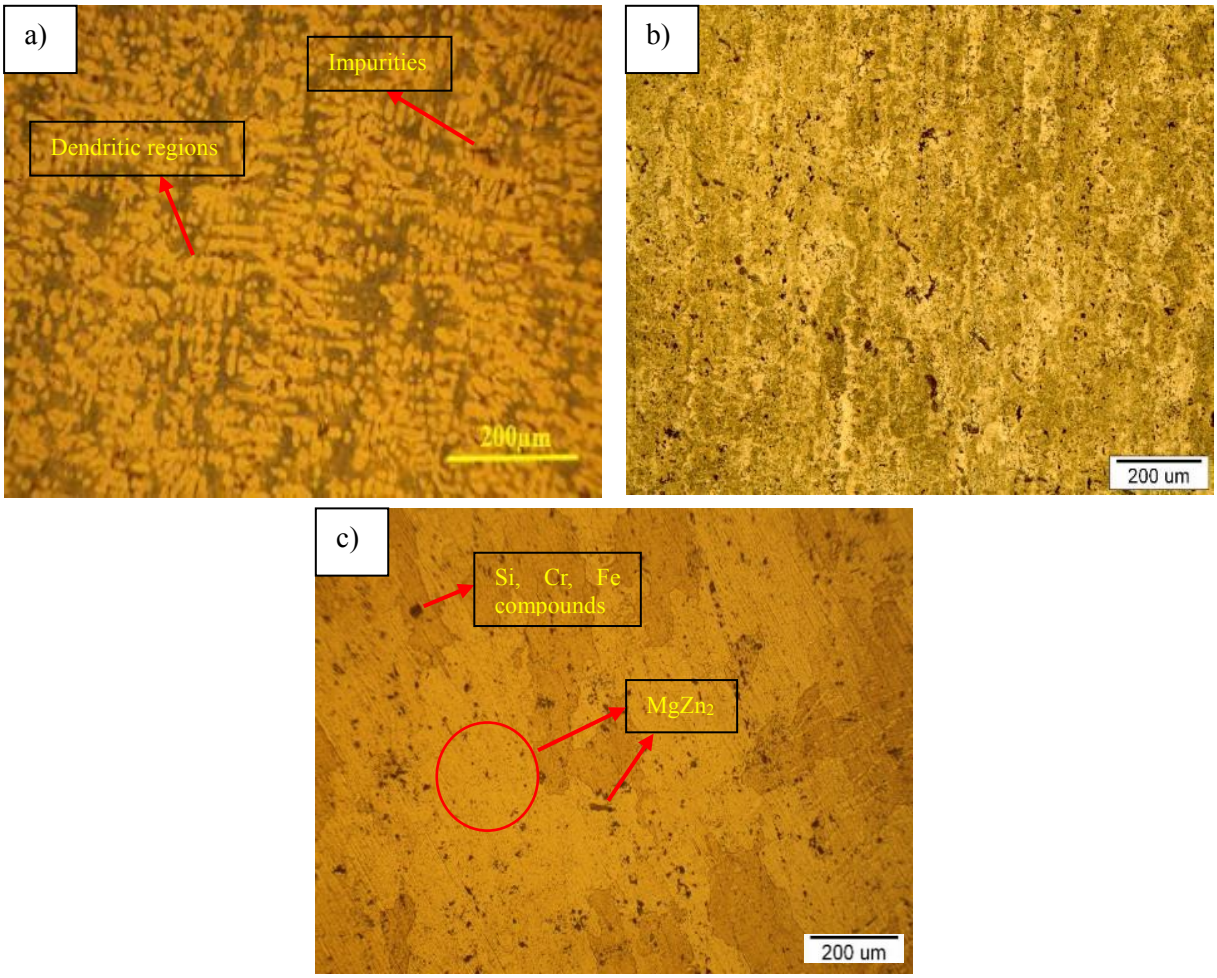

Fig. 3. The microstructure of a) as-cast, b) annealed, and c) heat-treated AA 7075 used in this research.

[DOI: 10.22068/ijmse.2578]

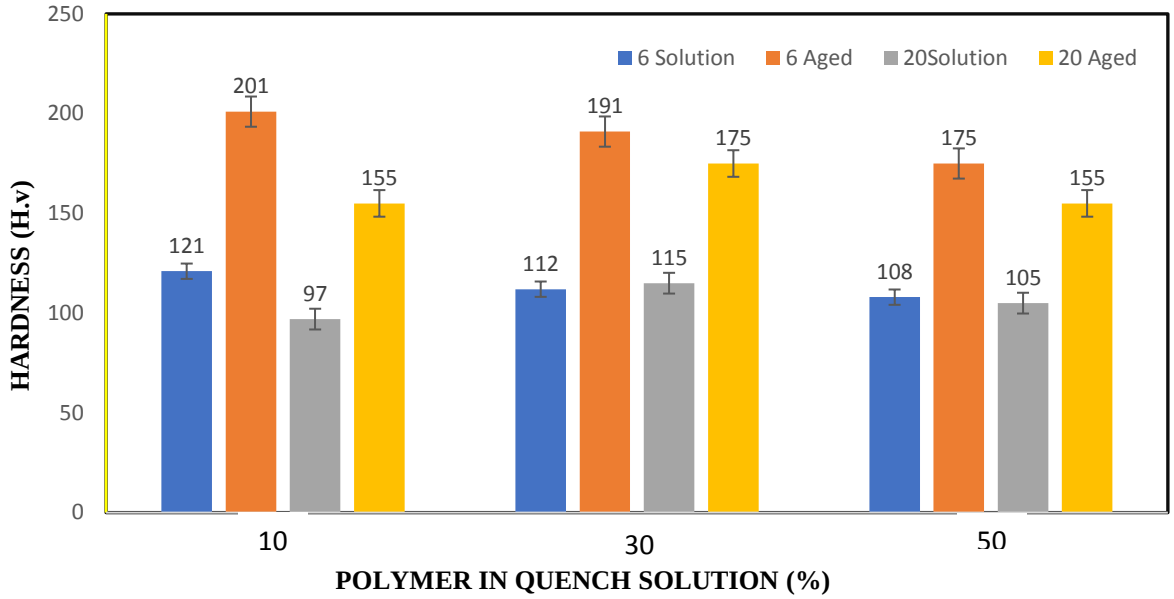

Fig. 4. The effect of different cooling environments on the hardness after solutionizing.

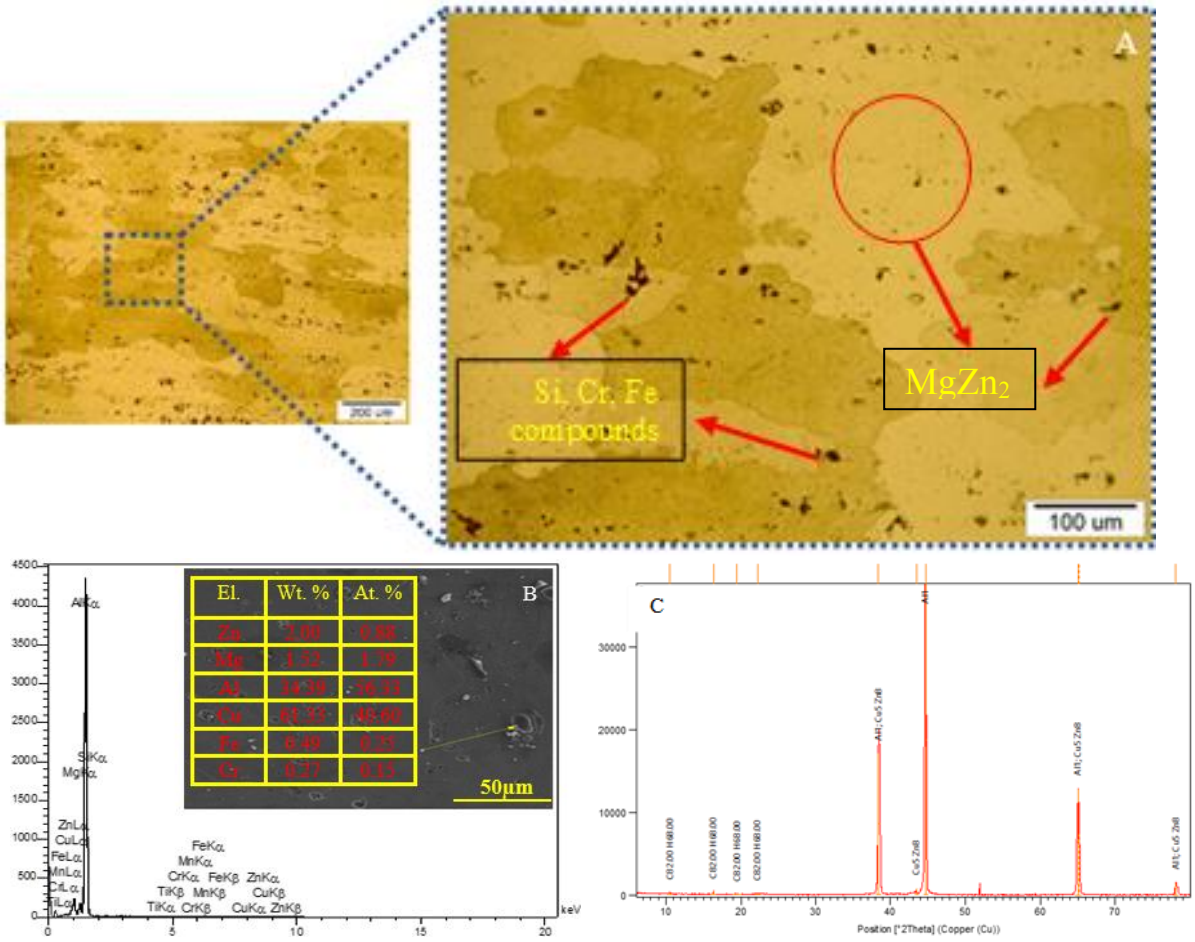

Fig. 5. Sample E A) OM image with different magnifications, B) FESEM image and result, C) XRD results

[DOI: 10.22068/ijmse.2578]

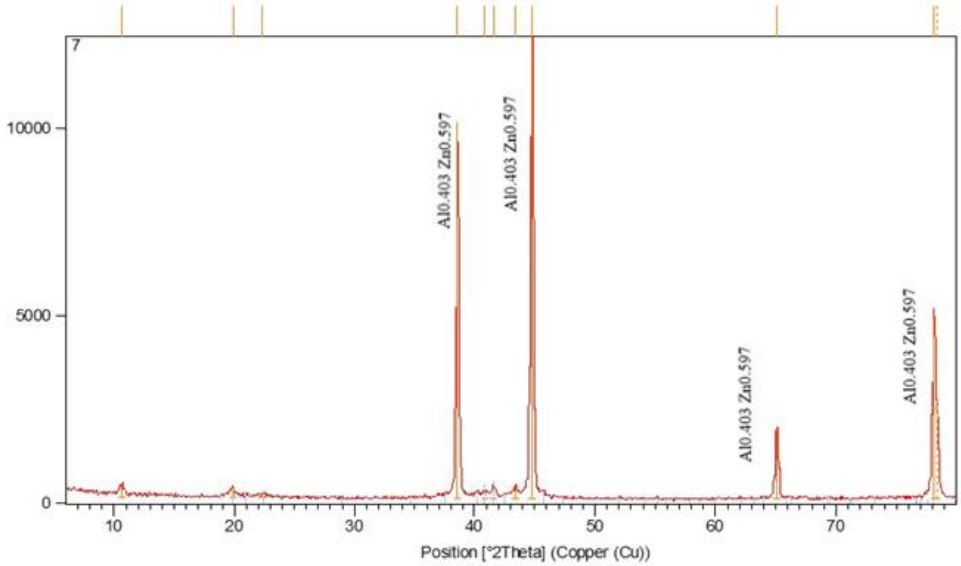

Fig. 6. The XRD results of solutionized and quenched sample H.

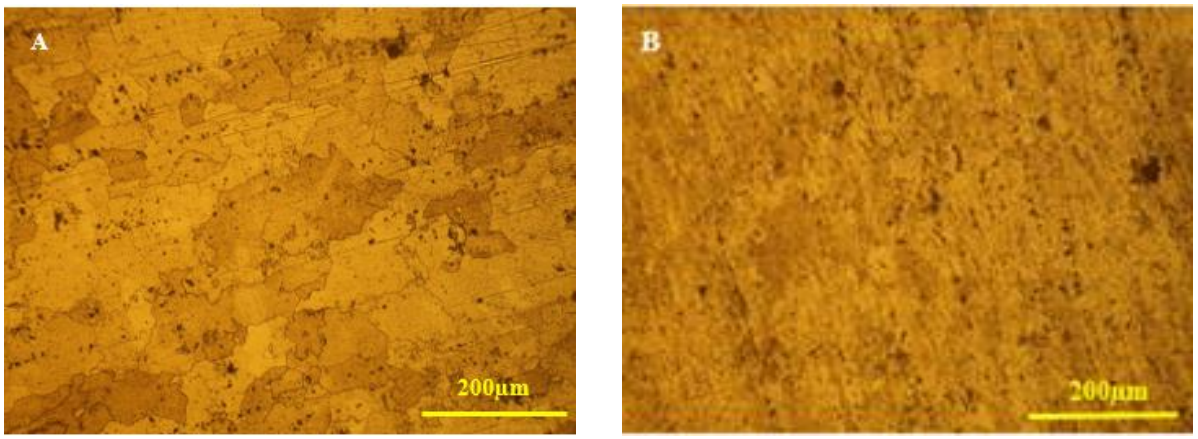

Fig. 7. AA7075 alloy solutionized and quenched in 30% polymer solution a) OM images of sample G; c) OM images of sample H

Due to the trace of Zn in XRD results, the accumulation of this element was because of the formation of Zn and Mg base precipitates after age-hardening.

The reason behind the increase in hardness can be credited to the greater diffusion of alloying elements. Based on the XRD results, the pre-aging OM images, and comparing them with Fig. 8, it can be seen that precipitates with a large and circular shape are Fe and Mg_2Si, which continued to grow. On the other hand, according to the yellow zones specified in Fig. 8 A and B, the small circular dots are $MgZn_2$ precipitates [6]. Based on OM images, the average grain size of 6- and 20-mm samples in different quenchants are represented in Figures 10 and Table 5.

According to previous research, the recrystallization temperature of AA7075 is between 185°C and 526°C. By placing Al at this temperature for 2 to 50 minutes can initiate the recrystallization process. Considering this, all samples exposed to the heat-treatment process at 285°C for 30 and 95 minutes underwent recrystallization, and in most of the matrix, the grain boundary has disappeared [16-24]. Incomplete recrystallization can increase the grain size, and, as can be seen in Table 5, the grain size of the 20 mm samples is larger than the 6 mm grain. The results of Table 6, Figure 9, EDS, XRD results, and hardness indicate that in 6 mm samples, the increase in Proof strength by decreasing the quench rate is the volume fraction

[DOI: 10.22068/ijmse.2578]

of the alloying elements [6, 9, 24]. However, as the quench rate decreased, 20 mm samples experienced a decrease in ultimate yield strength and proof strength, which can be attributed to the reduction in the volume fraction of the alloying elements. In low-thickness specimens, the elasticity limit was increased by decreasing the kench rate and decreasing the hardness.

Table 4. Possible phases formed in solid-solution of AA7075 [15].

IF Zn, Mg< 2.3%		
$MgZn_2$		Mg
IF Zn:Mg< 3%		Zn
$MgZn_2$	Mn_5ZnAl_{24}	
IF Cu< 1%		Cu
$Mg_3Zn_3Al_2$	$CuMgAl_2$	
IF Fe>Si , Cr>1/2 Fe	IF Fe>Si	Fe
$(FeCr)Al_7$	$FeAl_3$	
IF Cr>Si		Cr
$(CrFe)Al_7$		

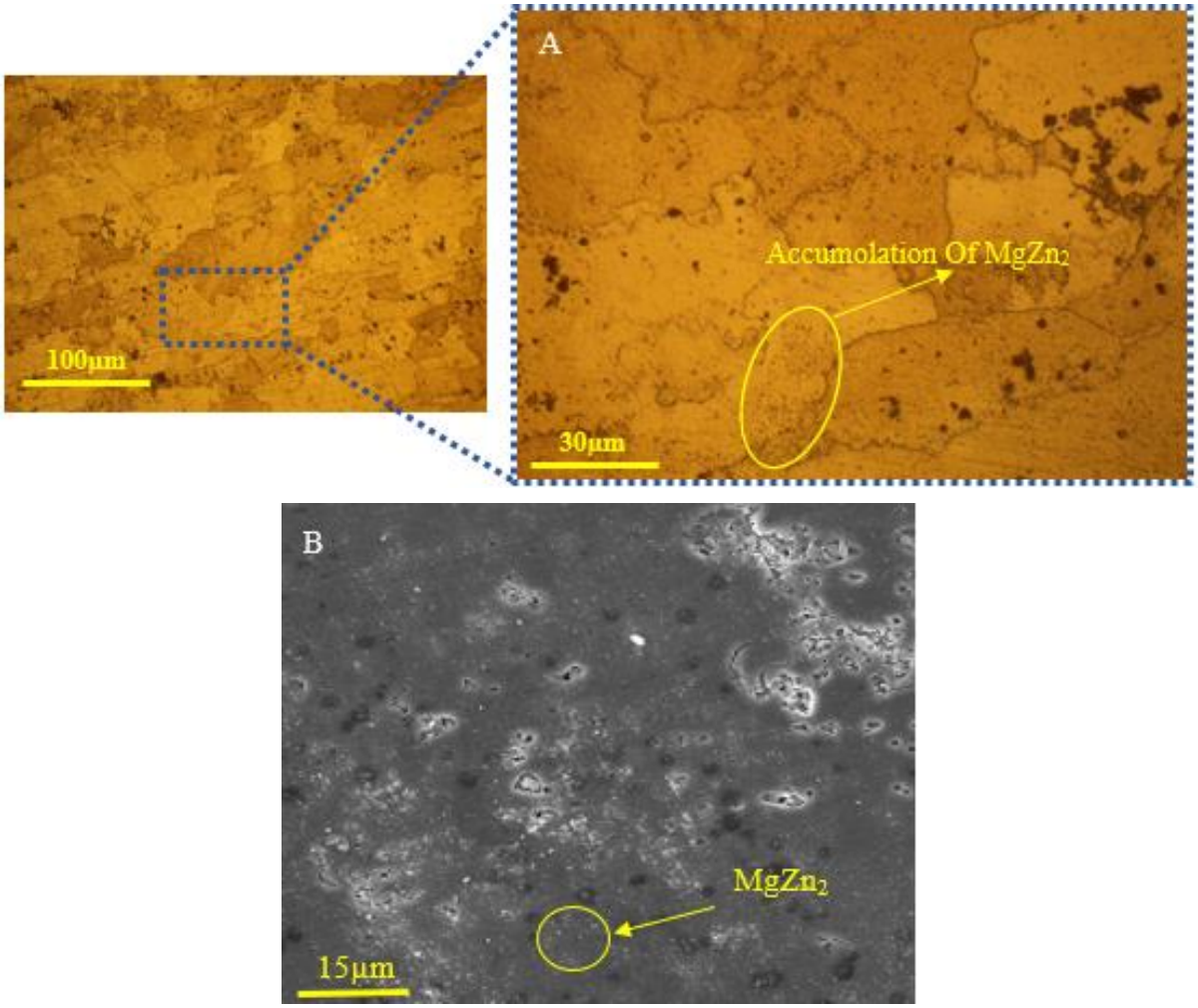

Fig. 8. The sample J after aging, A) OM images with different magnifications; C) FESEM image

[DOI: 10.22068/ijmse.2578]

Table 5. Grains' size

Sample's Code	Smallest Grain Size (µm)	Biggest Grain Size (µm)	Average Grain Size (µm)
A	169	545	345
B	200	787	416
C	35	148	85
D	--	--	--
E	145	1024	584
F	180	442	310
G	118	272	195
H	150	283	216
I	80	510	295
J	204	740	513

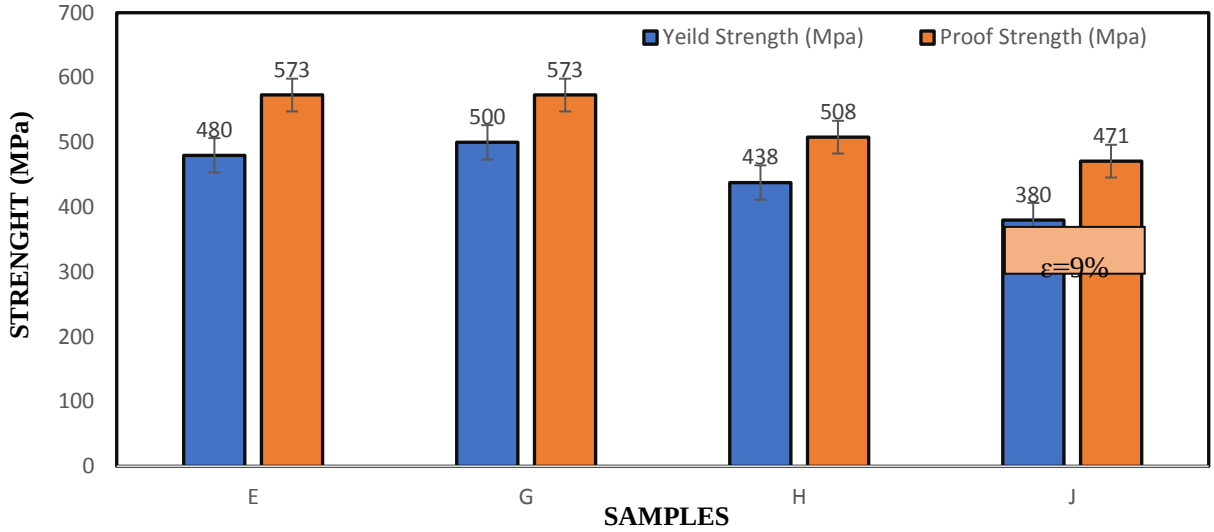

Fig. 1. The results of the samples' tensile test after age hardening.

4. CONCLUSIONS

The smelting and heat treatment processes of recycled 7075 aluminum alloy have been investigated in this paper. The microstructure, mechanical properties, and of recycled 7075 aluminum alloy were discussed, and the following conclusions can be seen:

1. The recycled 7075 aluminum alloys can be recovered, using swarf aluminum alloys as raw material. Non-aluminum such as impurities can be reduced by Martini N71P degasser tablets wrapped in aluminum foil and by holding it at the bottom of the cast to complete the deoxidation and degassing process.
2. After homogenization, solid solution, and aging treatment, the recycled 7075 aluminum alloy have more uniform composition distribution, finer grain, and better structure.
3. The hardness of the 6 mm thick samples decreased as the quench rate decreased, attributed to the decrease in the density of vacancies and dislocations due to their exit from the surface. The low hardness in samples with a thickness of 20 mm with a high quench rate could be because of the loss of grain boundaries and supersaturated solution.
4. The diffusion process of alloying elements, according to EDS, XRD, hardness, and tensile test results, indicates that as the Cr concentration increases, in high-energy areas, precipitate growth begins. Consequently, with the accumulation of elements such as Mg and Zn, the early stages of precipitates hardening of these alloy zones start.

REFERENCES

[1]. Das, S.K., Green, J.A., Kaufman, J.G., Emadi, D. and Mahfoud, M., "Aluminum recycling—An integrated, industrywide approach." JOM, 2010, 62, 23–26

[2]. Pan, X., Zhou, L., Wang, C., Yu, K., Zhu,

[DOI: 10.22068/ijmse.2578]

Y., Yi, M., Wang, L., Wen, S., He, W. and Liang, X., "Microstructure and residual stress modulation of 7075 aluminum alloy for improving fatigue performance by laser shock peening." IJMTM, 2023, 184, p.103979.

[3]. Croucher, T. "Using glycol to effectively control distortion and residual stresses in heat treated aluminum alloys." Journal of ASTM International, 2008.

[4]. Fontanari, V., Frendo, F., Rosellini, W. and Scardi, P., "Analysis of Residual Stress Distribution in Shot Peened AI 6082 T5 Alloy Subjected to Fatigue Loading." WIT Transactions on Engineering Sciences, 2001, 33.

[5]. Shang, B.C., Yin, Z.M., Wang, G., Liu, B. and Huang, Z.Q., "Investigation of quench sensitivity and transformation kinetics during isothermal treatment in 6082 aluminum alloy." Materials & Design, 2011, 32.7, 3818-3822.

[6]. Georgantzia, E., Gkantou, M. and Kamaris, G.S., "Aluminium alloys as structural material: A review of research." Engineering Structures, 2021, 227, 111372.

[7]. Hatch, John E., "Aluminium: Properties and Physical Metallurgy, by ASM." Metals Park, OH 135, 1984.

[8]. Rambabu, P.P.N.K.V., Eswara Prasad, N., Kutumbarao, V.V. and Wanhill, R.J.H., "Aluminium alloys for aerospace applications." Aerospace Materials and Material Technologies: Volume 1: Aerospace Materials, 2017, 29-52.

[9]. Suh, D.W., Lee, S.Y., Lee, K.H., Lim, S.K. and Oh, K.H., "Microstructural evolution of Al–Zn–Mg–Cu–(Sc) alloy during hot extrusion and heat treatments." Journal of Materials Processing Technology, 2004, 155, 1330-1336.

[10]. Zhou, B., Liu, B. and Zhang, S., "The advancement of 7xxx series aluminum alloys for aircraft structures: A review." Metals, 2021, 11.5., 718.

[11]. Handbook, A. S. M. "Vol. 20: Materials Selection and Design, ASM International." TA459.M43 1990 620.1'6 90-115, ISBN 0-87170-377-7 (v.1), 1997, pp. 811-819.

[12]. Greenwood, G.W. and Johnson, R.H., "The deformation of metals under small stresses during phase transformations." Proceedings of the Royal Society of London. Series A. Mathematical and Physical Sciences, 1965, 283. 1394, 403-422.

[13]. ASTM Standards, "ASTM B918 Vol 02.02, Standard Practice for Heat Treatment of Wrought Aluminum Alloys", ASTM International, 100 Barr Harbor Drive, POBoxC700, West Conshohocken, PA19428-2959. United State, 2020, PP 1-15.

[14]. Das, S.K. and Kaufman, J.G., "Recycling aluminum aerospace alloys." Advanced Materials and Processes, 2008, 166.3, 34.

[15]. Rosalie, J.M., Bourgeois, L. and Muddle, B.C., "Precipitate assemblies formed on dislocation loops in aluminium-silver-copper alloys." Philosophical Magazine, 2009, 89.25, 2195-2211.

[16]. Salman, J.M., Abd Alsada, S.A. and Al-Sultani, K.F., "Improvement properties of 7075-T6 aluminum alloy by quenching in 30% polyethylene glycol and addition 0.1% B." Research Journal of Material Sciences, 2013, ISSN 2320, 6055.

[17]. Ardell, A.J., "Precipitation hardening." Metallurgical Transactions A, 1985, 16, 2131-2165.

[18]. Totten, G.E. and MacKenzie, D.S. eds., "Handbook of aluminum: vol. 1: physical metallurgy and processes." CRC Press, 2003, page 305-350, 881-1062.

[19]. Soni, A., Samuel, A. and Prabhu, K.N., "Experimental investigation of heat transfer characteristics of polyethylene glycol (PEG) based quench media for industrial heat treatment." Experimental Thermal and Fluid Science, 2023, 144, 110865.

[20]. Tajally, M. and Huda, Z., "Recrystallization kinetics for aluminum alloy 7075." Metal science and heat treatment, 2011, 53, 213-217.

[21]. Shaeri, M.H., Shaeri, M., Ebrahimi, M., Salehi, M.T. and Seyyedein, S.H., "Effect of ECAP temperature on microstructure and mechanical properties of Al–Zn–Mg–Cu alloy." Progress in Natural Science: Materials International, 2016, 26.2, 182-191.

[22]. Younger, M.S. and Eckelmeyer, K.H.,

[DOI: 10.22068/ijmse.2578]

"Overcoming residual stresses and machining distortion in the production of aluminum alloy satellite boxes." No. SAND2007-6811. Sandia National Laboratories (SNL), Albuquerque, NM, and Livermore, CA (United States), 2007.

[23]. Keshavarzkermani, A., Esmaeilizadeh, R., Enrique, P.D., Asgari, H., Zhou, N.Y., Bonakdar, A. and Toyserkani, E., "Static recrystallization impact on grain structure and mechanical properties of heat-treated Hastelloy X produced via laser powder-bed fusion." Materials Characterization, 2021, 173, 110969.

[24]. Salvati, E., "Residual stress as a fracture toughening mechanism: A Phase-Field study on a brittle material." Theoretical and Applied Fracture Mechanics, 2021, 114, 103021.

[DOI: 10.22068/ijmse.2578]